Volume 11
Number 10
October 2025
Pages 2267–2470

Environmental Science
Water Research & Technology

rsc.li/es-water

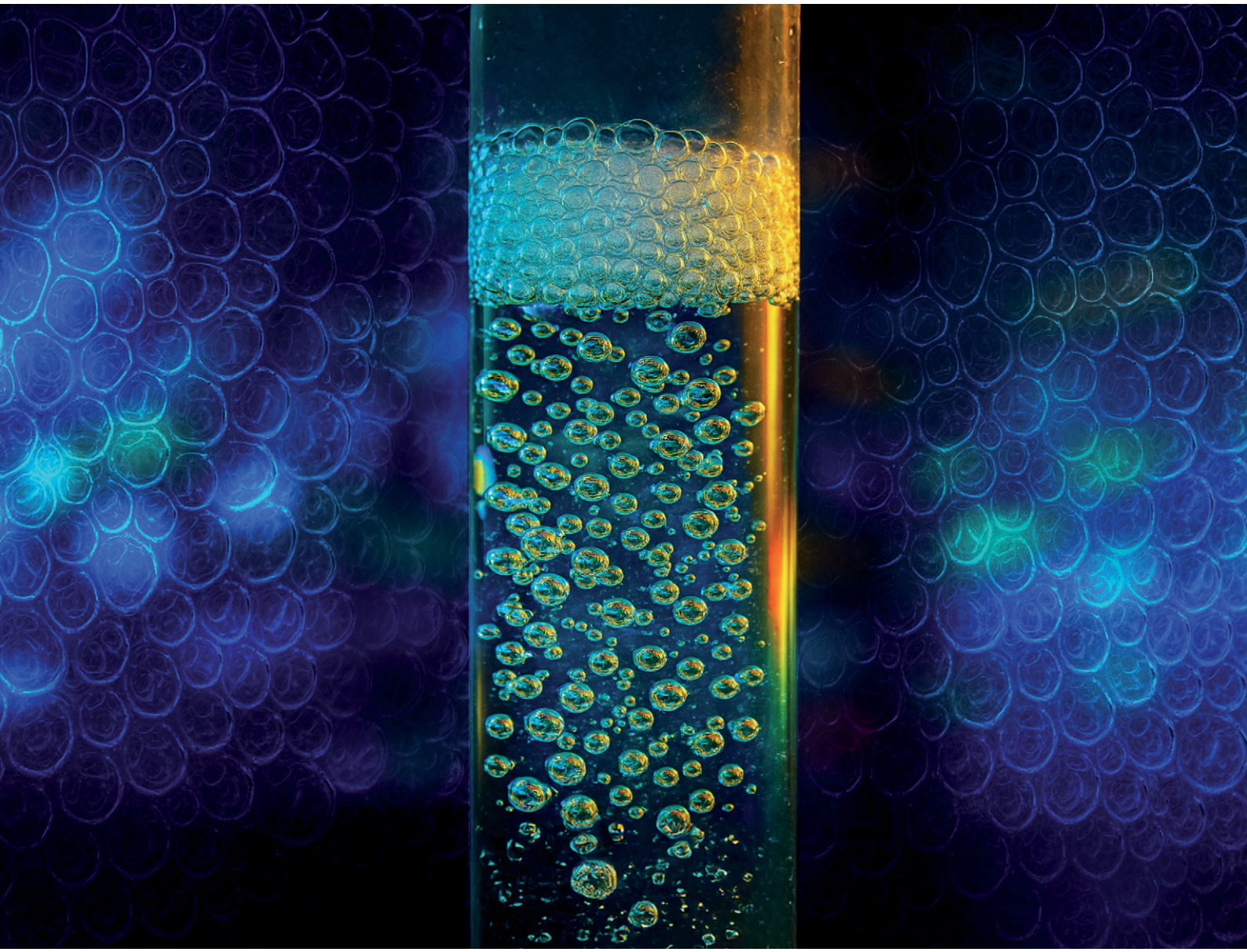

ISSN 2053-1400

ROYAL SOCIETY OF CHEMISTRY

PAPER
Kurt D. Pennell *et al.*
Removal of long- and short-chain PFAS from groundwater by foam fractionation

Environmental Science
Water Research & Technology

ROYAL SOCIETY OF CHEMISTRY

PAPER

View Article Online
View Journal | View Issue

Cite this: *Environ. Sci.: Water Res. Technol.*, 2025, **11**, 2295

Removal of long- and short-chain PFAS from groundwater by foam fractionation

Craig Klevan, Oren Van Allen, Kelly Mukai, Andre Gomes, Shana Xia, Seth Caines, Matthew J. Woodcock and Kurt D. Pennell *

Received 15th May 2025,
Accepted 25th July 2025

DOI: 10.1039/d5ew00440c

rsc.li/es-water

Due to the tendency for per- and polyfluoroalkyl substances (PFAS) to accumulate at the air–water interface, foam fractionation has gained attention as a cost-effective approach to treat PFAS-impacted water. Although foam fractionation is effective for long-chain length PFAS, short-chain PFAS are less surface active and can remain in solution even after extended treatment times. The objective of this study was to evaluate the ability of six cationic surfactants to remove both long- and short-chain length PFAS from groundwater by foam fractionation. Cetyltrimethylammonium bromide (CTAB) accumulated the most at the air–water interface and was subsequently evaluated in a foam fractionation system over a 4 order of magnitude range of PFAS concentrations, as well as 4 different CTAB mass delivery rates. For two natural groundwaters impacted by aqueous film forming foam (AFFF), total PFAS concentrations were reduced from ~15 000 ng L^{-1} to less than the detection limit of 8 ng L^{-1} in as short as 15 minutes. These findings demonstrate that the addition of CTAB, which exhibits a strong affinity for the air–water interface, to foam fractionation systems achieves rapid removal of both long- and short-chain PFAS from synthetic and natural groundwaters.

Water impact

Per- and polyfluoroalkyl substances (PFAS) concentrations in groundwater may span orders of magnitude. This work exhibits the versatility of cationic surfactant-enhanced foam fractionation over a range of long-chain and short-chain PFAS concentrations in groundwater including water contaminated with aqueous film-forming foam (AFFF) and provides key insights into avoiding spreading contamination through aerosolization and minimizing residual water pollution with cationic surfactants used for treatment.

1 Introduction

Per- and polyfluoroalkyl substances (PFAS) are a class of several thousand synthetic chemicals that have been manufactured since the 1940s and have become a global threat to human and environmental health.[1,2] These anthropogenic chemicals are characterized by strong C–F bonds that lead to beneficial properties such as chemical inertness and physical stability, but are also the reason these compounds persist in the environment, where they can be found in soil, water bodies, and biota.[3,4] Due to the widespread use of PFAS, there are ample opportunities for human exposure to PFAS, which can lead to adverse health effects such as damage to the kidneys and liver, as well as impaired fetal development.[5–7]

An important property of PFAS is their amphiphilic structure, which arises from a hydrophobic carbon fluorine chain and a hydrophilic head group, most commonly a carboxylic acid or sulfonic acid. This structure leads to surface active behavior, including accumulation at the air–water interface where the hydrophobic chain is oriented toward the nonpolar air and the hydrophilic head group is oriented toward the polar water.[8–10] The extent to which PFAS accumulate at interfaces is heavily dependent on the molecular structure of the individual PFAS compounds (*e.g.* head group, linear or branched), and for common anionic PFAS such of perfluoroalkyl carboxylic acids (PFCAs) and perfluoroalkyl sulfonic acids (PFSAs) is generally proportional to the length of the carbon–fluorine chain, with longer chain PFAS exhibiting greater hydrophobicity and greater accumulation at interfaces.[11,12] Shorter chain-length PFAS tend to exhibit less adsorption at interfaces, and therefore are often more mobile in the environment.[13,14]

Due to the tendency for many PFAS to accumulate at the air–water interface, foam fractionation has emerged as a promising method to remove PFAS from contaminated water. Foam fractionation involves the injection of air into the bottom of a vessel containing contaminated water, where PFAS then accumulate at the air–water interface of the air bubbles as they rise through the water column, with a goal of creating a PFAS-enriched foam at the top of the water column. Removal efficiencies for long-chain PFAS typically approach >90%, whereas short-chain PFAS may only achieve

Brown University, School of Engineering, Providence, RI, USA.
E-mail: kurt_pennell@brown.edu

removal efficiencies on the order of 5–50% due to their lower affinity for the air–water interface.[15–20] Foam fractionation operating conditions (*e.g.*, air flow rate, bubble size) can strongly influence PFAS removal efficiencies.[16,18,21,22] Likewise, the extent of PFAS accumulation at the air–water interface can be influenced by solution properties, such as ionic strength or competing species.[15,16,23]

Since most PFAS possess a negative charge in aqueous solutions, cationic surfactants, such as cetyltrimethylammonium bromide (CTAB), have been found to be effective in enhancing removal of short-chain PFAS.[15,17] Complex solutions, such as landfill leachate, have been shown to reduce the ability of cationic co-surfactants to enhance the removal of short-chain PFAS.[10,24–26] Due to these issues, it is often necessary to pilot test foam fractionation systems and adjust parameters until removal targets have been achieved. For example, the performance of CTAB with PFAS-impacted groundwater has not been extensively studied, nor has removal performance been demonstrated over a range of PFAS concentrations, in particular, dilute concentrations that are typically observed in groundwater plumes.[16]

Thus, the overall goal of this work was to evaluate the ability of six cationic co-surfactants (3 poly(diallyldimethylammonium chloride) (polyDADMAC) and 3 trimethylammonium compounds) to enhance the removal of both long- and short-chain PFAS during foam fractionation of synthetic and natural PFAS-impacted groundwaters. Surface tension data were measured for each co-surfactant, and this information was used to guide co-surfactant selection for foam fractionation tests with synthetic groundwater containing long- and short-chain PFAS over four orders of magnitude concentration range. Based on these results, foam fractionation with CTAB was evaluated using PFAS-impacted groundwater from two military installations, and at four mass flow rates to further explore system optimization.

2 Experimental/methods

2.1 Materials

2.1.1 Reagents. Two representative long-chain PFAS, perfluorooctanoic acid (PFOA) and perfluorooctanesulfonic acid potassium salt (K-PFOS) as well as two representative short-chain PFAS, perfluorobutanoic acid (PFBA) and perfluorobutanesulfonic acid potassium salt (K-PFBS) were used in experiments with synthetic groundwater. All PFAS compounds were obtained from Sigma Aldrich (St. Louis, MO). Cetyltrimethylammonium bromide (CTAB, $C_{19}H_{42}BrN$, CAS #: 57-09-0), Dodecyltrimethylammonium bromide (DTAB, $C_{15}H_{34}BrN$, CAS #: 1119-94-4), and Octyltrimethylammonium bromide (OTAB, $C_{21}H_{46}BrN$, CAS #: 2083-68-3) were purchased from Sigma Aldrich (St. Louis, MO). Solutions with PolyDADMAC of low, medium, and high molecular weights (<100 000 Da, 200 000–350 000 Da, 400 000–500 000 Da respectively) were purchased from Sigma Aldrich (St. Louis, MO). Polyquaternium-10 was purchased from Ninth Avenue (Bergen, Norway). Synthetic groundwater (SGW) with ionic strength 8.5 mM was used as the background solution for all surface tension and foam fractionation experiments unless otherwise specified and was prepared to match ionic compositions common in United States aquifers, containing 36 mg L^{-1} $MgSO_4$, 109 mg L^{-1} $NaHCO_3$,7 mg L^{-1} KCl, and 220 mg L^{-1} $CaCl_2$, all purchased from Fisher Scientific (Waltham, MA).[27] PFAS-impacted groundwater samples were obtained from the former Loring Air Force Base in Limestone, ME and a US Navy installation located in the eastern United States. Information regarding the properties of these groundwaters can be found in section SI: Experimental parameters. Methanol (LC-MS grade) was purchased from Honeywell (Charlotte, NC). Ultrapure MilliQ water (18 MΩ cm) was used for all solution preparations. Internal PFAS standards and calibration standards were purchased from Wellington Laboratories Inc. (Guelph, ON, Canada). Additional information related to the PFAS standards is provided in the SI section SII.

2.1.2 Foam fractionation apparatus. The experimental set-up for foam fractionation is consistent with our prior work.[28] The foam fractionation water column was constructed from a single piece acrylic tubing (ePlastics, Coppell, TX) with dimensions of 60 cm height and 5 cm diameter. The bottom of the acrylic column was threaded and fitted with a custom stainless-steel end plate that was threaded to accommodate an air sparger stone (0.5 μm pores and 1/4″ barb connection) and a drainage valve. Compressed laboratory air flowed through a pressure gauge (NOSHOK, Berea, OH) and an air-flow meter (King Instrument Company, Garden Grove, CA) before entering the endplate and air stone. Between the flow meter and the acrylic column, a custom-made water trap was inserted to protect the gauges from water that may enter through the air sparger. All connections were made with 1/4″ inside diameter Tygon™ tubing. The column contained two sampling ports along the height of the water column (15 cm and 30 cm from bottom) to sample in space. The ports were threaded into the acrylic column with a Luer-lock fitting septa (QOSINA, Ronkankoma, NY). The top of the acrylic column was equipped with an inverted funnel secured to vacuum tubing that leads to a vacuum pump (Welch, Ilmenau Germany) equipped with a vacuum pressure gauge (Ashcroft, Stratford, CT). Two 1000 mL Büchner flasks (Fisher Scientific, Waltham, MA) were placed between the column and the vacuum pump to trap foam removed from the system. The first flask was placed on a balance (Mettler Toledo, Columbus, OH) to monitor the foam removal rate, while the second flask is present as a safety factor to protect the vacuum pump if the foam were to overflow from the first flask. The discharge line from the vacuum pump was connected to flexible tubing and secured to the inside of a laboratory exhaust snorkel. There is also an additional port and valve (Hamilton Co, Reno, NV), located 8 cm from the bottom of the column to allow for additives to be pumped into the system with a Masterflex L/S ® peristaltic pump

(VWR, Radnor, PA). A schematic diagram of the foam fractionation apparatus is shown in Fig. 1.

2.2 Methods

2.2.1 Surface tension measurements. Surface tension measurements were obtained with a Sigma 700 precision force tensiometer (Biolin Scientific, Gothenburg, Sweden) equipped with a micro-roughened platinum Wilhelmy plate (Nanoscience Instruments, Phoenix, AZ). Solutions were prepared in 125 mL HDPE bottles by adding the necessary amounts of either co-compound or PFAS to synthetic groundwater. Prior to each surface tension measurement, the Wilhelmy plate was removed from the instrument micro-balance and rinsed with MilliQ water, followed by methanol, and then flamed with a butane torch until shining crimson in color to remove any impurities left from the previous experiment. Surface tension measurements were obtained for each solution with five replicate measurements per solution at room temperature (21.5 ± 1 °C). pH measurements were obtained using an Orion Star A221 pH Meter (Thermo Scientific, Waltham, MA) calibrated with buffer solutions at pH 4.01, 7.00 and 10.01 (Fisher Scientific, Waltham, MA).

2.2.2 Foam fractionation experiments. Experimental procedures are consistent with those in previous studies from our lab.[28] Prior to each foam fractionation experiment the acrylic column was thoroughly washed and rinsed with methanol and MilliQ water and air-dried. Fresh septa and sampling needles were utilized for each experiment. To minimize the presence of particulate matter, the groundwater collected from military sites was centrifuged in an Eppendorf 5804R benchtop centrifuge (Eppendorf, Hamburg, Germany) for 30 minutes at 4000 rpm. Each solution was sampled prior to adding to the system to obtain initial concentration of PFAS. The volume of solutions added was determined gravimetrically. An adsorption control experiment in which the solution sat in the system in the absence of aeration was performed to ensure that rapid removal of compounds is not due to adsorption to the system itself (Fig. S6).

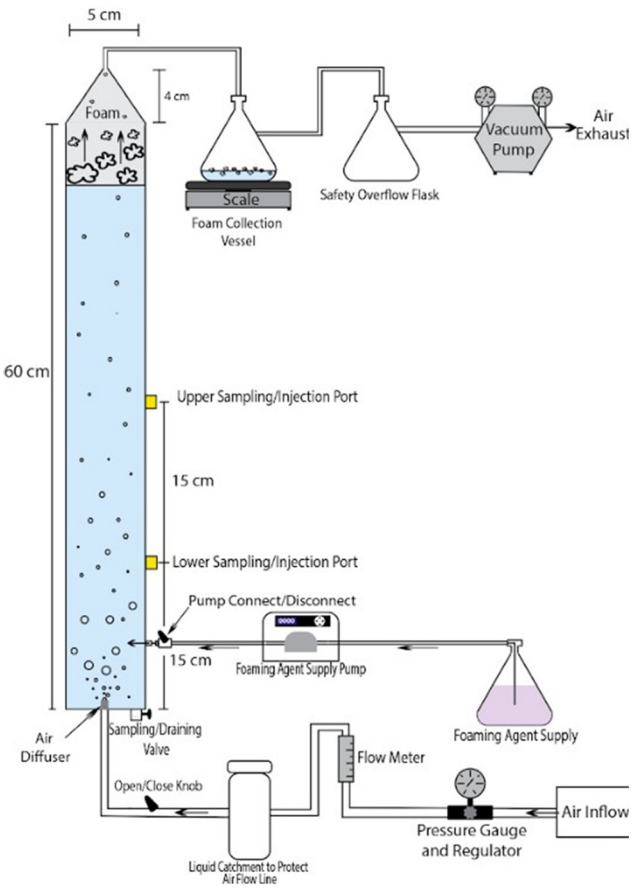

Fig. 1 Schematic diagram of the foam fractionation apparatus.

Foam fractionation experiments were carried out in semi-batch mode. For each experiment, the column was filled up to approximately 95% capacity (the true volume is recorded gravimetrically) with the synthetic groundwater containing mixtures or the AFFF impacted groundwater, after which an inverted funnel was quickly sealed to the top of the column to allow the column to operate under vacuum conditions. At the start of each experiment compressed air flow was initiated at the same time as the injection of a co-foaming agent if one was being used. The vacuum pump at this time was turned on to remove foam generated by the system. The time taken to add the solution to the system and turn on the equipment is less than 30 seconds. The experimental conditions, including air flow rate, air pressure, and vacuum pressure are summarized in the SI section SI: Experimental parameters. For each experiment, the foam fractionation system was operated for up to 2 hours, with ~1 mL samples collected in triplicate from the bottom and upper sampling ports in the water column at 2, 5, 10, 15, 20, 30, 40, 50, 60, 75, 90, 105, and 120 minutes of elapsed operation time with higher resolution early in the experiment as preliminary studies suggest this is when removal is most rapid. Foam generation was monitored over the duration of the experiment. At the conclusion of the experiment, the foam collapsed with the addition of methanol and then was diluted for subsequent quantification. Initial PFAS concentrations are provided in the SI section SI: Experimental parameters. Characteristics of bubbles were determined through image analysis with ImageJ as described in SI section SIII; Additional bubble and foam analysis.[29]

2.2.3 Analytical methods. PFAS quantification was analyzed using a Waters AQUITY H-Class ultra-performance liquid chromatography (UPLC) equipped with XEVO micro triple quadrupole mass spectrometry (TQS). Groundwater samples from AFFF impacted sites were analyzed using EPA Method 1633.[30] For experiments with synthetic groundwater containing only PFOA, PFOS, PFBA, and PFBS, samples and standards were prepared by addition of internal standard solution (10% V/V) in methanol (LC-MS grade, Honeywell, Charlotte, NC) with glacial acetic acid (1% V/V, Fisher Chemical, Fair Lawn, NJ). The methods used for samples prepared in synthetic groundwater are consistent with

recently published work from our lab.[28,31,32] Additional details for this analysis including instrument operation settings are in SII: Analytical Information.

3 Results and discussions

3.1 Accumulation of PFAS and co-foaming agents at the air–water interface

3.1.1 PFAS. Surface tension measurements were performed on two long-chain and two short-chain PFAS compounds in background solutions of synthetic groundwater as described in section 2.1.1. Similar to hydrocarbon surfactants, many PFAS tend to accumulate at the air–water interface and greater accumulation at the air–water interface is associated with greater reductions in the interfacial tension of water.[8,33] The concentration at which the surface tension starts to decrease is called the critical reference concentration (CRC) and the concentration where surface tension stops decreasing and remains constant with increasing soluble concentration corresponds to the critical micelle concentration (CMC).[10,23,34] Between these points, the concentration of compound at the air–water interface, the surface excess, can be estimated with the concentration *versus* surface tension data with the Gibbs equation (eqn (1)). These data may be fit to the Szyskowski equation to obtain fitted parameters '*a*' and '*b*', which are then substituted into the Gibbs equation to obtain the Langmuir/Szyskowski (L/S) equation used to predict the surface excess (Fig. S5).[8,32] Focusing on the Gibbs equation (eqn (1)), the surface excess (Γ, M L^{-2}) increases as more surface active species (*e.g.*, PFAS) accumulates at the air–water interface which is manifested as a reduction in surface tension (σ, M T^{-2}) with increasing concentration (C, M L^{-3}) in the bulk aqueous phase.

$$\Gamma = \frac{-1}{RT}\frac{\partial\sigma}{\partial \ln C} \quad (1)$$

Plots of surface tension data and corresponding L/S model fits for surface excess determination over concentration of two representative long-chain PFAS (PFOA, PFOS) and two representative short-chain PFAS (PFBA, PFBS) are shown in Fig. 2.

It is evident from Fig. 2 that long-chain PFAS such as PFOA (Fig. 2a) and PFOS (Fig. 2b) exhibit much greater accumulation to the air water interface than PFBS (Fig. 2c) and PFBA (Fig. 2d). Likewise, the sulfonic acid compounds (PFOS and PFBS) exhibit greater surface tension reduction relative to their analogous carboxylic acid compounds (PFOA and PFBA, respectively) at the same concentrations. The short-chain compounds only accumulate at the air–water interface enough to see a significant decrease in surface tension at concentrations several orders of magnitude higher than the concentration range relevant to the experiments in this study (Fig. S7). Furthermore, in mixtures, PFAS have been shown to exhibit competitive behavior at the air–water interface.[35–37] For example, in a system with limited adsorption sites and both PFOS and PFOA present, PFOS having greater interfacial affinity will outcompete PFOA for adsorption sites and may kick PFOA molecules off of the air–

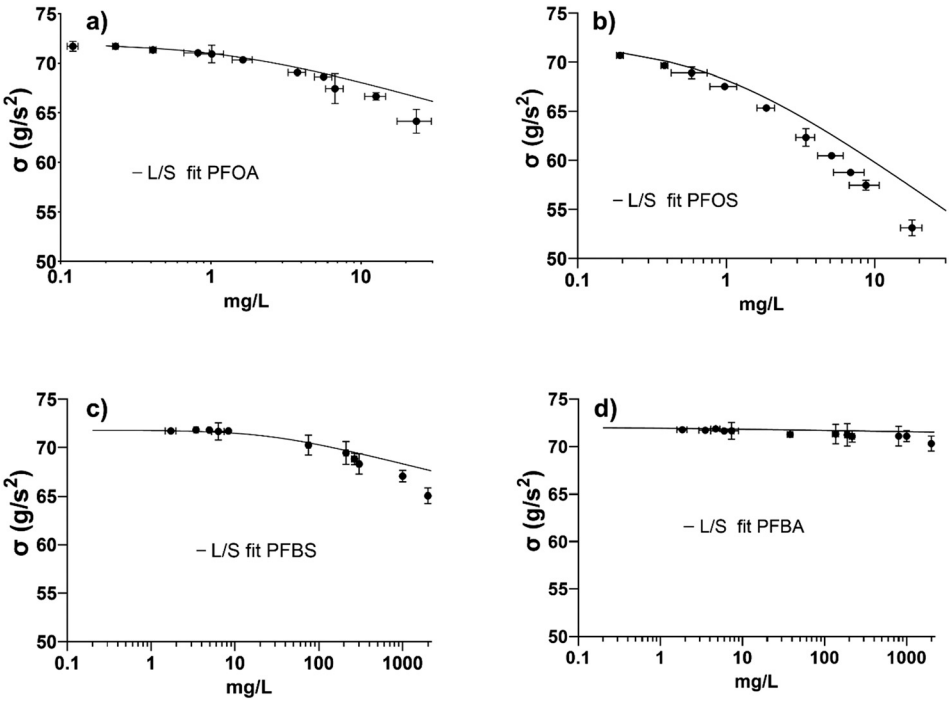

Fig. 2 Surface tension measurements and L/S model fits for 2 long-chain (PFOA, PFOS) and 2 short-chain (PFBS, PFBA) PFAS compounds in synthetic groundwater matrix. a) PFOA, b) PFOS, c) PFBS, d) PFBA. Vertical error bars represent standard deviation in surface tension data (n = 5 replicates) and horizontal data bars represent standard deviation in LC-MS measurements (n = 3 replicates). Points with missing error bars are due to symbols being larger than the error.

water interface.[32] Therefore, especially in mixtures with short-chain PFAS, these compounds may exhibit even less interfacial accumulation as the available interfacial area is preferentially occupied by long-chain PFAS.[38,39]

3.1.2 Co-foaming agents. Six cationic co-surfactants were tested for their affinity to the air–water interface, as it has been established that cationic surfactants are the most likely to enhance the removal of short-chain PFAS during foam fractionation.[17,25,40] Polydiallyldimethylammonium chloride (polyDADMAC) was tested as it is a commonly used cationic polyelectrolyte utilized in water treatment during the initial water clarification process.[41,42] OTAB (C_8TAB), DTAB (C_{12}TAB), and CTAB (C_{16}TAB) are common brominated cationic surfactants that are utilized in a variety of scientific and commercial applications. Changes in surface tension with increasing concentration of the candidate co-foaming agents are in Fig. 3. Based on the surface tension data, CTAB exhibited the greatest affinity to accumulate at the air–water interface, consistent with prior studies.[15,17,25,43] The resulting CMC for CTAB was approximately ~1 mM with a minimum ST of ~37 mN m^{-1}.[44,45] In contrast, the three polyDADMAC and the two shorter chain-length trimethylammonium bromides exhibited relatively minor reductions in surface tension over the concentration range tested, with no indication of micelle formation.

The observed differences in accumulation are important because cationic surfactants may interact with short-chain PFAS in the bulk aqueous phase and then accumulate as a pair to the air–water interface. Therefore, a cationic surfactant with high affinity for the air–water interface is likely to be more effective in removing short-chain PFAS during foam fractionation, compared to a cationic surfactant that exhibits lower surface activity.[17,40] As can been seen in Fig. 3, CTAB exhibits far greater surface activity than any of the other co-surfactants tested. Additionally, co-surfactants that strongly accumulate at air–water interface also support the formation of stable foams.[46] Foamability, the foam generation capacity, and foam stability, the lifetime of the foam, must be considered during foam fractionation. Likewise foam properties such as liquid content are important to consider as foam drainage may reintroduce PFAS back into the bulk liquid.[47–49] Foam consistency is explored further in the SI section: SIII: Additional bubble and foam analysis.

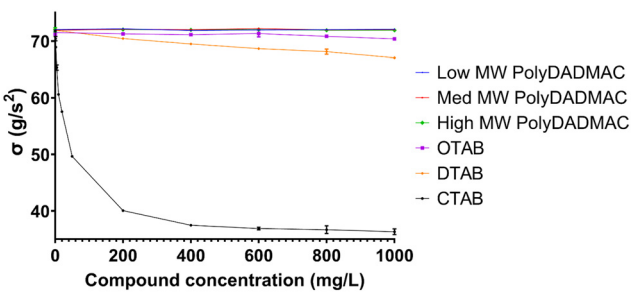

Fig. 3 Surface tension data for six potential cationic co-foaming agents in synthetic groundwater. Error bars represent standard deviation in surface tension data (n = 5 replicates). Missing error bars are due to symbols size being greater than the error.

3.2 Foam fractionation experiments

3.2.1 Control experiment. Based on the surface tension results shown in Fig. 3, CTAB was selected as the co-foaming agent for subsequent foam fractionation experiments. An initial foam fractionation experiment was performed to understand the removal of PFAS in synthetic groundwater with no co-surfactant present. Initial concentrations for each of the four PFAS compounds (PFOS, PFOA, PFBS, PFBA) were approximately 40 μg L^{-1}. All initial concentrations were confirmed by LC-MS/MS and are listed in Table S2. The long-chain PFAS (PFOS and PFOA) exhibited rapid removal, which plateaued at approximately 90% and 60%, respectively. The greater removal of PFOS compared to PFOA is consistent with their relative their surface excesses (Fig. S7) from the accumulation at the air–water interface determined from surface tension measurements (Fig. 2). PFBS and PFBA exhibited minimal removal in the absence of a co-foaming agent, which was expected due to their much lower affinity for the air–water interface. The system did not create foam in the absence of a co-surfactant, and therefore, removal was not due to foam fractionation, but instead due to aerosolization. PFAS enriched bubbles burst at the surface creating PFAS laden droplets that can either be removed, immediately fall back into solution, or re-enter the solution more slowly through adhering to the wall of the column and falling back into the matrix.[50,51] The steep initial removal for the surface-active compounds makes sense as at the earliest times the largest concentration gradient exists for mass transfer from the bulk solution to the air–water interface often modeled based off of first order kinetic removal.[52–54]

The small rises and falls in concentration of PFOS and PFOA resulting in a relatively flat portion of the curve after the first several minutes is likely due to the recycling of the PFAS in the system as the aerosolized droplets make their way back into the solution for the PFAS to then be removed again with the bubbles. In a similar nonfoaming system it was observed that PFAS reentering the matrix can cause the removal to seemingly halt and even cause the concentration in solution to rise again.[17] Similarly in a reactor with a larger radius droplets immediately reentered solution and although the more surface-active PFAS were adsorbing to the bubbles the removal appeared to be very minimal until the researchers placed a barrier over the system to capture the droplets and observed the expected removal behavior.[55] These results in the absence of co-foaming agent indicate that the droplets must be properly captured to keep track of PFAS mass and to avoid spread through spray or reentry into the system and that the co-foaming surfactant is necessary to capture the PFAS in a foam (Fig. 4).[21,56]

To enhance the removal of PFAS and generate sufficient foam to recover the removed PFAS mass, the foam fractionation system was operated under identical conditions

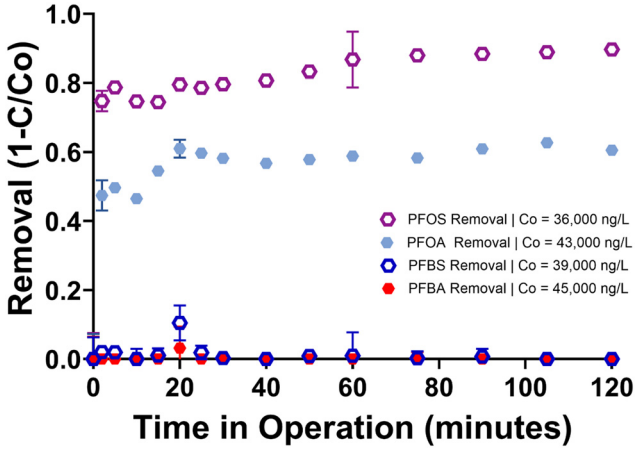

Fig. 4 Removal of a mixture of four PFAS (PFOS, PFOA, PFBS, and PFBA) from synthetic groundwater *via* air bubble injection. Error bars on this figure and all following figures represent standard deviation from triplicate sample taken at each time-step.

but with the addition of a peristaltic pump to supply CTAB as a co-foaming agent at a mass flow rate of 1 mg min^{-1} ($Q_{CTAB,in}$ = 1 mL min^{-1}). These conditions keep the water height approximately constant and any dilution due to the addition of the CTAB solution is negligible relative to the total volume of the system. The CTAB created a rich foam that was removed from the top of the column with a vacuum system. A less surface-active co-surfactant such as DTAB creates a bubbly liquid with a much higher liquid content which does not allow for concentration of the PFAS before removal (SI, section SIII). To ensure that the PFAS was being completely removed, both sampling ports were measured to monitor spatial PFAS concentration distribution within the system. As shown in Fig. 5a and b both the long-chain and short-chain PFAS were rapidly removed from the foam fractionation system. PFOA and PFOS achieved >99% removal in as short as five minutes, while the same level of removal was achieved for PFBS and PFBA after approximately 50 minutes of operation. The enhanced removal of PFOA and PFOS was attributed to the mechanisms associated with the introduction of CTAB into the system. As inferred from Fig. 3, the introduction of CTAB reduces the interfacial tension of the solution, which is directly proportional to bubble size allowing for stabilization and longer lifetimes of smaller bubbles.[57] The smaller bubbles provide increased surface area for adsorption, which is further explored in Section III of the SI. As the CTAB adsorbs to the bubble surfaces, the positive charges are on the outside of the bubble allowing for electrostatic repulsions between bubbles preventing merging, which in turn allows for a greater quantity of small bubbles available for the PFAS to adsorb.[58] (Fig. S2). Similarly, removal of PFBS and PFBA was enhanced due to the greater interfacial area, coupled with interaction with CTAB, and subsequent migration to the air–water interface as an ion pair.[17,18,59]

3.2.2 Effects of initial PFAS concentration on removal. To demonstrate that foam fractionation would be effective over a wide range of PFAS concentrations, the four PFAS were tested in the synthetic groundwater at individual concentrations ranging from 400 ng L^{-1} (0.4 μg L^{-1}) to 400 000 ng L^{-1} (400 μg L^{-1}). As shown in Fig. 5a, the long-chain PFAS (PFOS and PFOA) exhibited near complete removal in as short as 5 minutes. Fig. 6 shows that the removal profiles for these compounds obtained at different initial PFAS concentrations were nearly identical, indicating that the chosen operation parameters for the system will remove long-chain PFAS similarly over a three order of magnitude concentration range. The removal efficiencies for PFBS and PFBA are shown in Fig. 6a and b, respectively.

The PFAS removal profiles for each concentration were similar, indicating that the mass flow rate of CTAB was sufficient for removal of PFAS in concentrations up to orders of magnitude far greater than the typically observed in contaminated surface water and groundwater.[60,61] The lowest PFAS concentration mixture resulted in the steepest initial removal of PFBS and PFBA. The 99% removal achieved for the highest concentration values corresponds to approximately ~335 μg mass of each PFAS and required the same amount of time as the lowest concentration, where approximately 335 ng of each PFAS was removed. At the highest PFAS concentration tested, the total PFAS in the system amounted to ~4.16 μmol, with 2.68 μmol

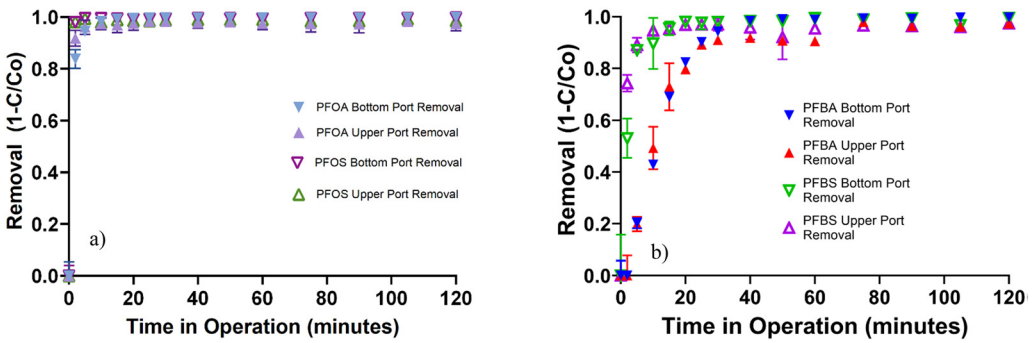

Fig. 5 Removal of an equal concentration PFAS mixture (PFOS | Co = 47 000 ng L^{-1}, PFOA | Co = 39 000 ng L^{-1}, PFBS | Co = 41 000 ng L^{-1}, PFBA | Co = 37 000 ng L^{-1}) from synthetic groundwater using foam fractionation with a CTAB feed rate of 1 mg min^{-1}. Fig. 5a) shows removal for PFOA and PFOS and Fig. 5b) shows removal for PFBA and PFBS.

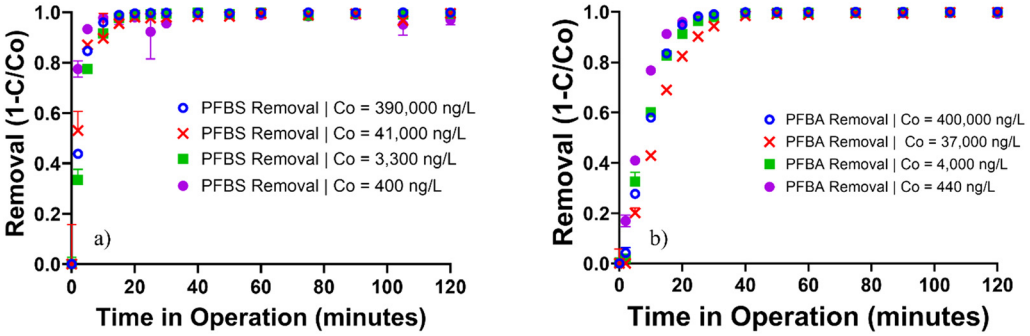

Fig. 6 Removal of a) PFBS and b) PFBA from synthetic groundwater in a foam fractionation system over four orders of magnitude concentration of PFAS in four compound mixture with a CTAB feed rate of 1 mg min^{-1}. Concentrations are averaged from measurements at both sampling ports as there was minimal concentration variations between ports.

representing PFBS and PFBA. The mass flow of CTAB corresponds to 3.5 μmol of the cetrimonium cation entering the system each minute, and therefore, a sufficient number of CTAB molecules were present to interact with short-chain PFAS. The quantity of CTAB entering the system is explored further in section 3.2.4.

3.2.3 Removal of PFAS from AFFF-impacted groundwater. Since the foam fractionation system worked well over a wide range of PFAS concentrations, the synthetic groundwater was substituted with groundwater obtained from two military installations with a history of aqueous film-forming foam (AFFF) usage. The properties of these waters, as well as the measured PFAS concentrations using EPA Method 1633 can be found in Tables S3 and S4 of section SI: Experimental parameters.[30] The elevated concentrations of PFOS and PFHxS detected in these groundwater samples are consistent with the composition of historically used electrochemical fluorination (ECF) produced AFFF.[62,63]

The results of the foam fractionation tests conducted with two different AFFF-impacted groundwaters are shown in Fig. 7 and S8–S11. Similar to the synthetic groundwater systems, PFBA was the slowest to be removed by the foam fractionation system in both groundwaters despite PFBA accounting for ~2% of the total PFAS concentration. The faster removal of PFAS from the former Loring Air Force Base compared to the second military installation was attributed to lower initial PFAS concentration as the solution properties for the two groundwaters were similar (Tables S3 and S4). However, it should be noted that aqueous chemistry can affect PFAS removal by foam fractionation even in the presence of a cationic co-surfactants such as CTAB.[15,18,25] For example, the optimal ratio for CTAB : PFAS may depend on the ionic strength and the ionic composition of the aqueous matrix.[59] The solution pH and ionic composition are also important to consider as the CTAB interactions may be enhanced at lower pH, while in the foam ions present may compete with PFAS for CTAB assisted removal and influence the foam stability due to electrostatic screening effects.[64–66] While the system employed here worked well for the two AFFF-impacted groundwaters, it may be less effective in matrices that are more complex or that contain antifoaming constituents.[25]

3.2.4 Effect of CTAB dosage. Although the foam fractionation system worked well in the experiments reported above, it may be beneficial to reduce the CTAB dose to save material costs. Therefore, the experiment reported in Fig. 5 was repeated with lower CTAB dosing rates of 0.5 mg min^{-1}, 0.1 mg min^{-1}, and 0.05 mg min^{-1} compared to the 1 mg

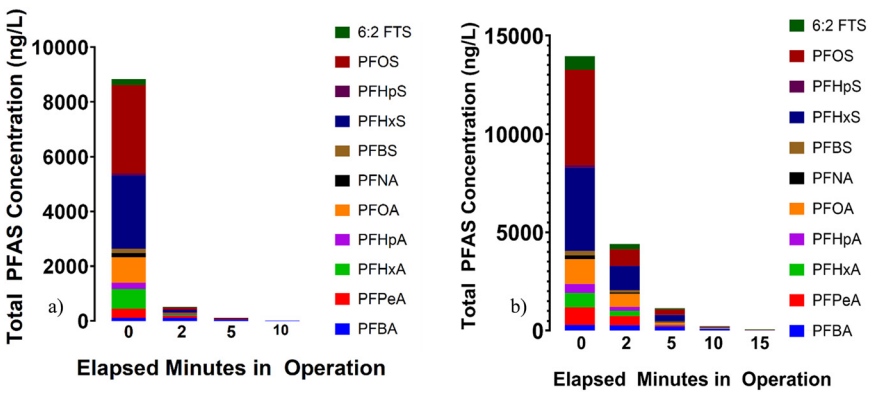

Fig. 7 Removal of PFAS from groundwaters obtained from a) the former Loring Air Force Base in Limestone, ME and b) a military installation located in the eastern United States. Concentrations are averaged from measurements at both sampling ports as there was minimal concentration variations between ports. Plots of removal for each PFAS species are provided in section SIV.

min^{-1} dosing rate used previously. The removal of PFOS and PFOA exhibited the same rapid removal curve displayed in Fig. 5a regardless of the dosing rate, and therefore, we will focus on PFBS and PFBA removal as a function of CTAB dosage. As shown in Fig. 8a, the dosage of CTAB had little influence on the removal of PFBS from foam fractionation system, which achieved 99% removal of PFBS after 10 minutes of operation. The initial PFBS concentration in all cases was approximately 40 μg L^{-1} (0.11 μM), while the lowest CTAB mass delivery rate (0.05 mg min^{-1}) translates to 0.175 μmoles of the cationic cetrimonium ion entering the system each minute. Thus, if the CTAB and PFBS interaction occurs at 1–1 ratio, there was sufficient CTAB available in the system after only 1 minute of operation.

The results shown in Fig. 8b indicate less favorable removal of PFBA compared to the other PFAS species, which decreased as the CTAB delivery rate was reduced from 0.5 mg min^{-1} to 0.1 mg min^{-1}. However, there are several other optimization parameters to be considered. Cost is always important to consider in a system such as the one used in this study would increase with increased CTAB dosing as the material used increases linearly with time (Fig. 9a). Along with PFAS removal, other metrics for foam fractionation success include volume reduction factors (VRFs), PFAS enrichment factors (EF), and mass recovery. VRF is the ratio of the volume of solution to be treated to the volume of collapsed foam at the termination of a foam fractionation run. For a compound of interest, the EF is the ratio of the concentration of that species in the foamate to the concentration of the compound in the initial solution and would be equal to the VRF if removal and recovery were both 100%. For instance, if a goal were to treat 1000 L of water containing to 4000 ng L^{-1} of PFOA to a volume of 10 L and have a remaining concentration of 4 ng L^{-1} to comply with EPA maximum concentration levels (MCL) the VRF would be 100 and the EF would be 99.9 assuming all removed PFAS mass ends in the foamate. However, if only 70% of the removed mass was detected in the foamate the VRF would still be 100 and the EF would be 69.93. Solely reporting removal may be misleading, as removal may appear high, but without a stable foam the solution may simply be transferred from one vessel to another and the VRF would be extremely low, resulting in an overall ineffective process (Fig. S5).

From examination of the results at the various dosing rates there are several trends evident. The higher doses lead to increases in removed foam and in turn lower VRF and EF as the larger quantity of extracted liquid dilutes the removed PFAS. This is common in foam fractionation as there is typically a tradeoff between achieving either greater enrichment *versus* greater recovery.[67] The enrichment factor can be improved by simply stopping the system earlier when there is maximum removal with less foam, or by performing secondary foam fractionation on the initial generated foam to further concentrate in a smaller volume, but this may lead to additional costs.[68] While the dosing rate of the 1 mg min^{-1} results in the lowest VRF and EF, the ratio between these values for is ~1 for this dosing rate and the ratio decreases as dosing rate decreases indicating that the higher dosing rate leads to the greatest recovery. This is likely because the higher dosing rate creates a stable foam able to retain the PFAS the most rapidly as opposed to lower dosing rates where it would take longer for the CTAB to be able to coat the bubble surfaces efficiently enough to create a stable foam, and until this point the experiment, in the absence of stable foam, the behavior is more similar to the control experiment with no CTAB where there is removal of PFAS yet no recovery. Since the VRF is an order of magnitude higher than the recovery, the EF for the lower dosing rates is still far higher than for the higher dosing rates despite the lesser PFAS recovery. This may potentially be mitigated by premixing CTAB with the PFAS prior to initiating aeration allowing for rapid formation of stable foam even with a low CTAB dose rate. Therefore, when optimizing a foam fractionation system, the tradeoffs between removal, material costs, operation time, foam volume generated, and treatment costs should be considered.

4 Conclusions

This work highlights methods to overcome low removal of short-chain PFAS during foam fractionation through addition of cationic co-surfactants. The initial control experiment demonstrated that while bubble flotation in the absence of

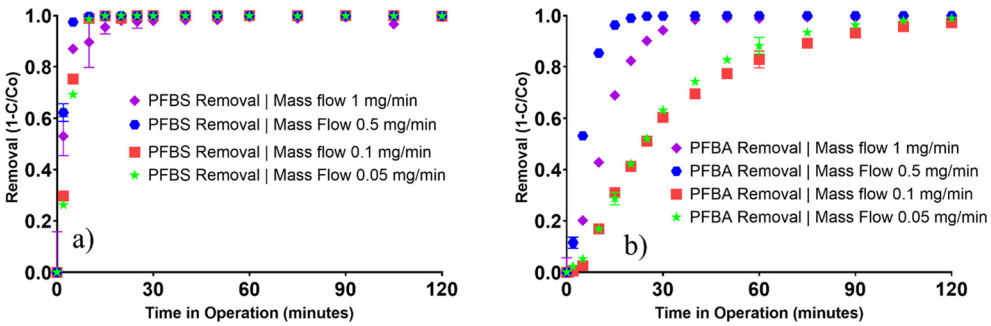

Fig. 8 Removal of a) PFBS and b) PFBA from contaminated synthetic groundwater at four different mass flow rates of CTAB. Concentrations are averaged from measurements at both sampling ports as there was minimal concentration variations between ports.

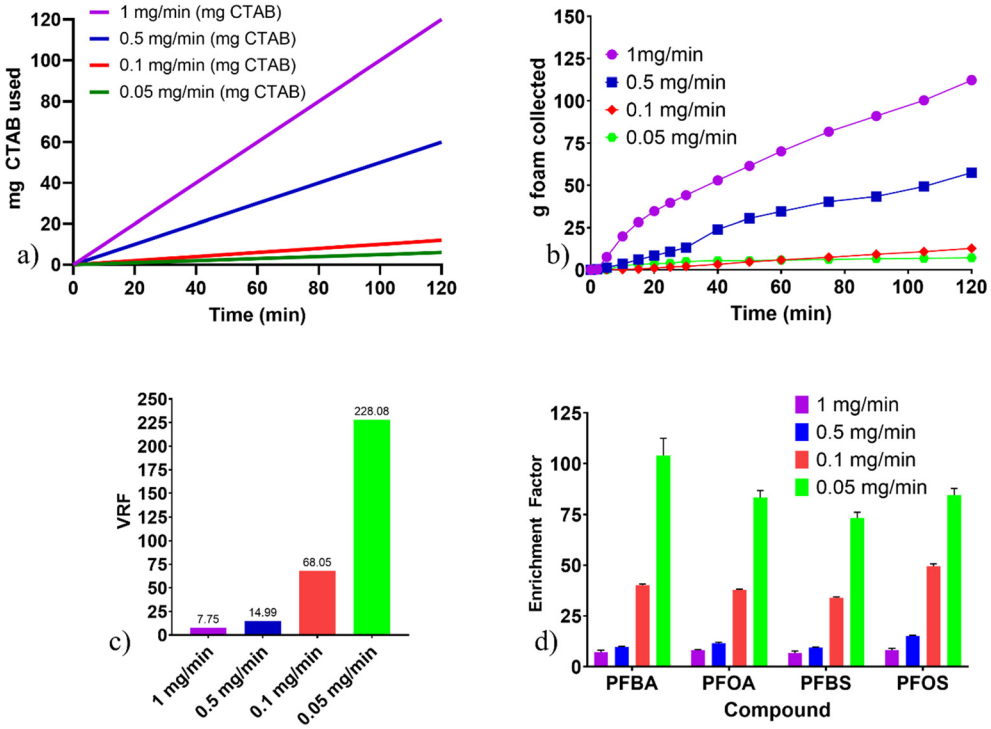

Fig. 9 Additional considerations to optimize the foam fractionation system for PFAS removal with CTAB as a co-surfactant a) CTAB material usage, b) collected foam over time c) volume reduction factor at end of experiment (120 min) and d) enrichment factors for each PFAS species. Error bars are due to the standard deviations in influent concentration (n = 3 replicate measurements) and standard deviations in foamate concentration (n = 3 replicate measurements) in calculation of the enrichment factor.

co-surfactant can be effective for removing long-chain PFAS (>60% removal for PFOA and >90% removal for PFOS), it will be necessary to capture the PFAS spread through the bursting of bubbles at the water surface to complete mass balances and to avoid potential losses of PFAS to the atmosphere during treatment.[17,55,56] Of the cationic co-surfactants tested, CTAB was found to be highly effective at removing both long- and short-chain PFAS over a wide range of aqueous phase concentrations. The success of CTAB compared to other cationic co-surfactants in the foam fractionation system was consistent with the surface tension reductions and corresponding accumulation at the air–water interface, which can be used as screening approach during the selection of co-surfactants for foam fractionation. For example, DTAB, which exhibited minimal changes in surface tension, may appear to generate foam, but instead, the process forms a bubbly liquid with minimal enrichment. Furthermore, this work illustrates the tradeoffs encountered when selecting co-surfactants dosage rate as material costs, operation time, and foam volume must all be considered. While CTAB was very effective at removing PFAS from the AFFF impacted groundwaters, there have been reports of CTAB being less effective from more complex aqueous matrices such as landfill leachate.[25] Furthermore, CTAB is known to exhibit aquatic toxicity, and thus, further research should be undertaken to identify alternatives to CTAB, and CTAB residual concentrations should be monitored to assess potential exposure risk.[69,70]

Author contributions

Craig Klevan: conceptualization, methodology, validation, formal analysis, investigation, resources, writing – original draft, writing – review & editing, visualization, supervision, project administration Oren Van Allen: methodology, validation, investigation, writing – review & editing, visualization Shana Xia: methodology, investigation, writing – review & editing, visualization Kelly Mukai: methodology, investigation, writing – review & editing, visualization Andre Gomes: methodology, investigation, writing – review & editing, visualization Seth Caines: methodology, investigation, writing – review & editing, visualization Matthew Woodcock: formal analysis, resources, writing – review & editing Kurt Pennell: conceptualization, writing – original draft, writing – review & editing, supervision, project administration, funding acquisition.

Conflicts of interest

Kurt Pennell and Craig Klevan are listed as inventors on a pending patent application # 63/777,267 which involves additives to improve foam fractionation.

Data availability

The data supporting this article have been included as part of the SI.

Supplementary information is available: The content of the supplementary information includes experimental parameters, details on analytical methods, additional discussion of bubble and foam analyses, as well as plots explaining adsorption control experiments, surface excess predictions and individual compound removal curves for PFAS present in the AFFF-impacted groundwater. See DOI: https://doi.org/10.1039/D5EW00440C.

Acknowledgements

Support for this research was provided by the Strategic Environmental Research and Development Program (SERDP) under Project ER21-3540 (contract number W912HQ-23-C-0031): "Polymer Addition for Improved Removal of Short-Chain PFAS by Dissolved Air Flotation". The content of this manuscript has not undergone SERDP review, and no official endorsement should be inferred. The authors would also like to acknowledge Max Karnik for assistance with preliminary laboratory tasks as well as Brown University 'Joint Engineering and Physical Instrument Shop' machinists Michael Packer, Donald Wright, and James Carroll for assistance with construction of the foam fractionation apparatus. We would also like to thank Mr. Naji Akladiss for assisting with the collection of groundwater from the former Loring Air Force Base in Limestone, ME.

References

1 S. Moavenzadeh Ghaznavi, C. Zimmerman, M. E. Shea, J. D. MacRae, J. M. Peckenham, C. L. Noblet, O. G. Apul and A. D. Kopec, Management of Per- and Polyfluoroalkyl Substances (PFAS)-Laden Wastewater Sludge in Maine: Perspectives on a Wicked Problem, *Biointerphases*, 2023, **18**(4), 041004, DOI: 10.1116/6.0002796.

2 G. M. Sinclair, S. M. Long and O. A. H. Jones, What Are the Effects of PFAS Exposure at Environmentally Relevant Concentrations?, *Chemosphere*, 2020, **258**, 127340, DOI: 10.1016/j.chemosphere.2020.127340.

3 C. Ng, I. T. Cousins, J. C. DeWitt, J. Glüge, G. Goldenman, D. Herzke, R. Lohmann, M. Miller, S. Patton, M. Scheringer, X. Trier and Z. Wang, Addressing Urgent Questions for PFAS in the 21st Century, *Environ. Sci. Technol.*, 2021, **55**(19), 12755–12765, DOI: 10.1021/acs.est.1c03386.

4 M. G. Evich, M. J. B. Davis, J. P. McCord, B. Acrey, J. A. Awkerman, D. R. U. Knappe, A. B. Lindstrom, T. F. Speth, C. Tebes-Stevens, M. J. Strynar, Z. Wang, E. J. Weber, W. M. Henderson and J. W. Washington, Per- and Polyfluoroalkyl Substances in the Environment, *Science*, 2022, **375**(6580), eabg9065, DOI: 10.1126/science.abg9065.

5 S. E. Fenton, A. Ducatman, A. Boobis, J. C. DeWitt, C. Lau, C. Ng, J. S. Smith and S. M. Roberts, Per- and Polyfluoroalkyl Substance Toxicity and Human Health Review: Current State of Knowledge and Strategies for Informing Future Research, *Environ. Toxicol. Chem.*, 2021, **40**(3), 606–630, DOI: 10.1002/etc.4890.

6 L. J. L. Espartero, M. Yamada, J. Ford, G. Owens, T. Prow and A. Juhasz, Health-Related Toxicity of Emerging per- and Polyfluoroalkyl Substances: Comparison to Legacy PFOS and PFOA, *Environ. Res.*, 2022, **212**, 113431, DOI: 10.1016/j.envres.2022.113431.

7 E. National Academies of Sciences, H. and M. Division, D. on E. and L. Studies, B. on P. H. and P. H. Practice, B. on E. S. Toxicology and C. on the G. on P. T. Outcomes and H. Potential Health Effects of PFAS, in *Guidance on PFAS Exposure, Testing, and Clinical Follow-Up*, National Academies Press, US, 2022.

8 J. Costanza, M. Arshadi, L. M. Abriola and K. D. Pennell, Accumulation of PFOA and PFOS at the Air–Water Interface, *Environ. Sci. Technol. Lett.*, 2019, **6**(8), 487–491, DOI: 10.1021/acs.estlett.9b00355.

9 Y.-M. Tricot, Surfactants: Static and Dynamic Surface Tension, in *Liquid Film Coating: Scientific principles and their technological implications*, ed. S. F. Kistler and P. M. Schweizer, Springer Netherlands, Dordrecht, 1997, pp. 99–136, DOI: 10.1007/978-94-011-5342-3_4.

10 K. Lunkenheimer, K. Geggel and D. Prescher, Role of Counterion in the Adsorption Behavior of 1:1 Ionic Surfactants at Fluid Interfaces—Adsorption Properties of Alkali Perfluoro-n-Octanoates at the Air/Water Interface, *Langmuir*, 2017, **33**(39), 10216–10224, DOI: 10.1021/acs.langmuir.7b00786.

11 M. L. Brusseau, QSPR-Based Prediction of Air–water Interfacial Adsorption Coefficients for Nonionic PFAS with Large Headgroups, *Chemosphere*, 2023, **340**, 139960, DOI: 10.1016/j.chemosphere.2023.139960.

12 J. F. Stults, Y. J. Choi, C. Rockwell, C. E. Schaefer, D. D. Nguyen, D. R. U. Knappe, T. H. Illangasekare and C. P. Higgins, Predicting Concentration- and Ionic-Strength-Dependent Air–Water Interfacial Partitioning Parameters of PFASs Using Quantitative Structure–Property Relationships (QSPRs), *Environ. Sci. Technol.*, 2023, **57**(13), 5203–5215, DOI: 10.1021/acs.est.2c07316.

13 S. C. E. Leung, D. Wanninayake, D. Chen, N.-T. Nguyen and Q. Li, Physicochemical Properties and Interactions of Perfluoroalkyl Substances (PFAS) - Challenges and Opportunities in Sensing and Remediation, *Sci. Total Environ.*, 2023, **905**, 166764, DOI: 10.1016/j.scitotenv.2023.166764.

14 W. Cai, D. A. Navarro, J. Du, G. Ying, B. Yang, M. J. McLaughlin and R. S. Kookana, Increasing Ionic Strength and Valency of Cations Enhance Sorption through Hydrophobic Interactions of PFAS with Soil Surfaces, *Sci. Total Environ.*, 2022, **817**, 152975, DOI: 10.1016/j.scitotenv.2022.152975.

15 T. Buckley, X. Xu, V. Rudolph, M. Firouzi and P. Shukla, Review of Foam Fractionation as a Water Treatment Technology, *Sep. Sci. Technol.*, 2022, **57**(6), 929–958, DOI: 10.1080/01496395.2021.1946698.

16 P. Meng, S. Deng, A. Maimaiti, B. Wang, J. Huang, Y. Wang, I. T. Cousins and G. Yu, Efficient Removal of Perfluorooctane Sulfonate from Aqueous Film-Forming Foam Solution by Aeration-Foam Collection, *Chemosphere*, 2018, **203**, 263–270, DOI: 10.1016/j.chemosphere.2018.03.183.

17 C.-S. Lee and A. K. Venkatesan, Cationic Surfactant-Assisted Foam Fractionation Enhances the Removal of Short-Chain Perfluoroalkyl Substances from Impacted Water, *Chemosphere*, 2024, **362**, 142614, DOI: **10.1016/j.chemosphere.2024.142614**.

18 A. C. E. We, A. Zamyadi, A. D. Stickland, B. O. Clarke and S. Freguia, A Review of Foam Fractionation for the Removal of Per- and Polyfluoroalkyl Substances (PFAS) from Aqueous Matrices, *J. Hazard. Mater.*, 2024, **465**, 133182, DOI: **10.1016/j.jhazmat.2023.133182**.

19 Y. Wang, Y. Ji, V. Tishchenko and Q. Huang, Removing Per- and Polyfluoroalkyl Substances (PFAS) in Water by Foam Fractionation, *Chemosphere*, 2023, **311**, 137004, DOI: **10.1016/j.chemosphere.2022.137004**.

20 M. Hiraide, Foam Fractionation And Flotation, in *Encyclopedia of Analytical Science*, ed. P. Worsfold, A. Townshend and C. Poole, Elsevier, Oxford, 2nd edn, 2005, pp. 195–201, DOI: **10.1016/B0-12-369397-7/00174-6**.

21 I. Ebersbach, S. M. Ludwig, M. Constapel and H.-W. Kling, An Alternative Treatment Method for Fluorosurfactant-Containing Wastewater by Aerosol-Mediated Separation, *Water Res.*, 2016, **101**, 333–340, DOI: **10.1016/j.watres.2016.05.063**.

22 N. A. Kazakis, A. A. Mouza and S. V. Paras, Experimental Study of Bubble Formation at Metal Porous Spargers: Effect of Liquid Properties and Sparger Characteristics on the Initial Bubble Size Distribution, *Chem. Eng. J.*, 2008, **137**(2), 265–281, DOI: **10.1016/j.cej.2007.04.040**.

23 C. Klevan, S. Caines, A. Gomes and K. D. Pennell, Accurate Determination of Perfluorooctanoate Aqueous Solubility, Critical Micelle Concentration, and Acid Dissociation Constant, *Environ. Sci. Technol. Lett.*, 2024, acs.estlett.4c00858, DOI: **10.1021/acs.estlett.4c00858**.

24 Y.-C. Lee, P.-Y. Wang, S.-L. Lo and C. P. Huang, Recovery of Perfluorooctane Sulfonate (PFOS) and Perfluorooctanoate (PFOA) from Dilute Water Solution by Foam Flotation, *Sep. Purif. Technol.*, 2017, **173**, 280–285, DOI: **10.1016/j.seppur.2016.09.012**.

25 P. H. N. Vo, T. Buckley, X. Xu, T. M. H. Nguyen, V. Rudolph and P. Shukla, Foam Fractionation of Per- and Polyfluoroalkyl Substances (PFASs) in Landfill Leachate Using Different Cosurfactants, *Chemosphere*, 2023, **310**, 136869, DOI: **10.1016/j.chemosphere.2022.136869**.

26 M. L. Brusseau and S. Van Glubt, The Influence of Surfactant and Solution Composition on PFAS Adsorption at Fluid-Fluid Interfaces, *Water Res.*, 2019, **161**, 17–26, DOI: **10.1016/j.watres.2019.05.095**.

27 L. A. DeSimone, P. B. McMahon and M. R. Rosen, *Water Quality in Principal Aquifers of the United States, 1991–2010*, Circular; Circular 1360, United States Geological Survey, 2015, p. 161.

28 C. Klevan, O. Van Allen, S. Xia, K. Mukai, A. Gomes, S. Caines, M. J. Woodcock and K. D. Pennell, Evaluation of Co-Foaming Agents for Enhanced Removal of Per-and Polyfluoroalkyl Substances (PFAS) by Foam Fractionation, *J. Hazard. Mater.*, 2025, 138423, DOI: **10.1016/j.jhazmat.2025.138423**.

29 C. A. Schneider, W. S. Rasband and K. W. Eliceiri, NIH Image to ImageJ: 25 Years of Image Analysis, *Nat. Methods*, 2012, **9**(7), 671–675, DOI: **10.1038/nmeth.2089**.

30 EPA, U.S. Environmental Protection Agency, *Method 1633A, Analysis of Per- and Polyfluoroalkyl Substances (PFAS) in Aqueous, Solid, Biosolids, and Tissue Samples by LC-MS/MS*, 2024, EPA 821-D-24-001, **https://www.epa.gov/cwa-methods/cwa-analytical-methods-and-polyfluorinated-alkyl-substances-pfas**.

31 S. Liao, M. Arshadi, M. J. Woodcock, Z. S. S. L. Saleeba, D. Pinchbeck, C. Liu, N. L. Cápiro, L. M. Abriola and K. D. Pennell, Influence of Residual Nonaqueous-Phase Liquids (NAPLs) on the Transport and Retention of Perfluoroalkyl Substances, *Environ. Sci. Technol.*, 2022, **56**(12), 7976–7985, DOI: **10.1021/acs.est.2c00858**.

32 U. Garza-Rubalcava, C. Klevan, K. D. Pennell and L. M. Abriola, Transport and Competitive Interfacial Adsorption of PFOA and PFOS in Unsaturated Porous Media: Experiments and Modeling, *Water Res.*, 2025, **268**, 122728, DOI: **10.1016/j.watres.2024.122728**.

33 E. Kissa, Fluorinated Surfactants and Repellents: Second Edition, Revised and Expanded Surfactant Science Series. Volume 97. By Erik Kissa (Consultant, Wilmington, DE). Marcel Dekker: New York. 2001. Xiv + 616 Pp. $195.00. ISBN 0-8247-0472-X, *J. Am. Chem. Soc.*, 2001, **123**(36), 8882, DOI: **10.1021/ja015260a**.

34 M. L. Brusseau, Examining the Robustness and Concentration Dependency of PFAS Air–water and NAPL-Water Interfacial Adsorption Coefficients, *Water Res.*, 2021, **190**, 116778, DOI: **10.1016/j.watres.2020.116778**.

35 W. Wang, X. Mi, Z. Zhou, S. Zhou, C. Li, X. Hu, D. Qi and S. Deng, Novel Insights into the Competitive Adsorption Behavior and Mechanism of Per- and Polyfluoroalkyl Substances on the Anion-Exchange Resin, *J. Colloid Interface Sci.*, 2019, **557**, 655–663, DOI: **10.1016/j.jcis.2019.09.066**.

36 J. E. F. Abraham, K. G. Mumford, D. J. Patch and K. P. Weber, Retention of PFOS and PFOA Mixtures by Trapped Gas Bubbles in Porous Media, *Environ. Sci. Technol.*, 2022, **56**(22), 15489–15498, DOI: **10.1021/acs.est.2c00882**.

37 X. Lyu, Z. Li, D. Wang, Q. Zhang, B. Gao, Y. Sun and J. Wu, Transport of Perfluorooctanoic Acid in Unsaturated Porous Media Mediated by SDBS, *J. Hydrol.*, 2022, **607**, 127479, DOI: **10.1016/j.jhydrol.2022.127479**.

38 B. Guo, H. Saleem and M. L. Brusseau, Predicting Interfacial Tension and Adsorption at Fluid–Fluid Interfaces for Mixtures of PFAS and/or Hydrocarbon Surfactants, *Environ. Sci. Technol.*, 2023, **57**(21), 8044–8052, DOI: **10.1021/acs.est.2c08601**.

39 J. A. K. Silva, W. A. Martin and J. E. McCray, Air–water Interfacial Adsorption Coefficients for PFAS When Present as a Multi-Component Mixture, *J. Contam. Hydrol.*, 2021, **236**, 103731, DOI: **10.1016/j.jconhyd.2020.103731**.

40 T. Buckley, K. Karanam, H. Han, H. N. P. Vo, P. Shukla, M. Firouzi and V. Rudolph, Effect of Different Co-Foaming Agents on PFAS Removal from the Environment by Foam Fractionation, *Water Res.*, 2023, **230**, 119532, DOI: **10.1016/j.watres.2022.119532**.

41 I. W. Mwangi, J. C. Ngila, P. Ndungu and T. A. M. Msagati, Method Development for the Determination of Diallyldimethylammonium Chloride at Trace Levels by Epoxidation Process, *Water, Air, Soil Pollut.*, 2013, **224**(9), 1638, DOI: **10.1007/s11270-013-1638-6**.

42 D. An, Y. Chen, B. Gu, P. Westerhoff, D. Hanigan, P. Herckes, N. Fischer, S. Donovan, J. P. Croue and A. Atkinson, Lower Molecular Weight Fractions of PolyDADMAC Coagulants Disproportionately Contribute to N-Nitrosodimethylamine Formation during Water Treatment, *Water Res.*, 2019, **150**, 466–472, DOI: **10.1016/j.watres.2018.12.002**.

43 P. Stevenson and S. I. Karakashev, Commercial-scale Removal of Short-chain PFAS in a Batch-wise Adsorptive Bubble Separation Process by Dosing with Cationic Co-surfactant, *Remediation*, 2024, **34**(1), e21767, DOI: **10.1002/rem.21767**.

44 S. Tiwari, C. Mall and P. P. Solanki, CMC Studies of CTAB, SLS & Tween 80 by Spectral and Conductivity Methodology to Explore Its Potential in Photogalvanic Cell, *Surf. Interfaces*, 2020, **18**, 100427, DOI: **10.1016/j.surfin.2019.100427**.

45 W. Li, M. Zhang, J. Zhang and Y. Han, Self-Assembly of Cetyl Trimethylammonium Bromide in Ethanol-Water Mixtures, *Front. Chem. China.*, 2006, **1**(4), 438–442, DOI: **10.1007/s11458-006-0069-y**.

46 M. J. Rosen and J. T. Kunjappu, *Surfactants and Interfacial Phenomena*, John Wiley & Sons, 2012.

47 S. Tcholakova and B. Petkova, Bubble Size and Foamability: Role of Surfactants and Hydrodynamic Conditions, *Curr. Opin. Colloid Interface Sci.*, 2024, **72**, 101824, DOI: **10.1016/j.cocis.2024.101824**.

48 A. Verma, N. Kumar and R. Raj, Direct Prediction of Foamability of Aqueous Surfactant Solutions Using Property Values, *J. Mol. Liq.*, 2021, **323**, 114635, DOI: **10.1016/j.molliq.2020.114635**.

49 S. A. Koehler, S. Hilgenfeldt and H. A. Stone, A Generalized View of Foam Drainage: Experiment and Theory, *Langmuir*, 2000, **16**(15), 6327–6341, DOI: **10.1021/la9913147**.

50 Y. Cao, C. Lee, E. T. J. Davis, W. Si, F. Wang, S. Trimpin and L. Luo, 1000-Fold Preconcentration of Per- and Polyfluorinated Alkyl Substances within 10 Minutes via Electrochemical Aerosol Formation, *Anal. Chem.*, 2019, **91**(22), 14352–14358, DOI: **10.1021/acs.analchem.9b02758**.

51 C. Lee, T. Yang, Y. Yao, J. Li and C. Huang, Rapid Detection of Perfluorinated Sulfonic Acids through Preconcentration by Bubble Bursting and Surface-assisted Laser Desorption/Ionization, *J. Mass Spectrom.*, 2021, **56**(4), e4667, DOI: **10.1002/jms.4667**.

52 J. Wang, R. K. Niven, A. Morrison, S. P. Wilson, V. Strezov and M. P. Taylor, Kinetic Model of PFAS Removal by Semi-Batch Foam Fractionation and Validation by Experimental Data for K-PFOS, *Sci. Total Environ.*, 2023, **865**, 161145, DOI: **10.1016/j.scitotenv.2022.161145**.

53 A. L. Morrison, V. Strezov, R. K. Niven, M. P. Taylor, S. P. Wilson, J. Wang, D. J. Burns and P. J. C. Murphy, Impact of Salinity and Temperature on Removal of PFAS Species from Water by Aeration in the Absence of Additional Surfactants: A Novel Application of Green Chemistry Using Adsorptive Bubble Fractionation, *Ind. Eng. Chem. Res.*, 2023, **62**(13), 5635–5645, DOI: **10.1021/acs.iecr.3c00150**.

54 S. Chen, M. B. Timmons, J. J. Bisogni and D. J. Aneshansley, Modeling Surfactant Removal in Foam Fractionation: I — Theoretical Development, *Aquac. Eng.*, 1994, **13**(3), 163–181.

55 D. Nguyen, J. Stults, J. Devon, E. Novak, H. Lanza, Y. Choi, L. Lee and C. E. Schaefer, Removal of Per- and Polyfluoroalkyl Substances from Wastewater via Aerosol Capture, *J. Hazard. Mater.*, 2024, **465**, 133460, DOI: **10.1016/j.jhazmat.2024.133460**.

56 S. J. Smith, J. Lewis, K. Wiberg, E. Wall and L. Ahrens, Foam Fractionation for Removal of Per- and Polyfluoroalkyl Substances: Towards Closing the Mass Balance, *Sci. Total Environ.*, 2023, **871**, 162050, DOI: **10.1016/j.scitotenv.2023.162050**.

57 M. Matsumoto and K. Tanaka, Nano Bubble—Size Dependence of Surface Tension and inside Pressure, *Fluid Dyn. Res.*, 2008, **40**(7–8), 546, DOI: **10.1016/j.fluiddyn.2007.12.006**.

58 Y. Xing, M. Xu, M. Li, W. Jin, Y. Cao and X. Gui, Role of DTAB and SDS in Bubble-Particle Attachment: AFM Force Measurement, Attachment Behaviour Visualization, and Contact Angle Study, *Minerals*, 2018, **8**(8), 349, DOI: **10.3390/min8080349**.

59 R. Li, O. F. Isowamwen, K. C. Ross, T. M. Holsen and S. M. Thagard, PFAS–CTAB Complexation and Its Role on the Removal of PFAS from a Lab-Prepared Water and a Reverse Osmosis Reject Water Using a Plasma Reactor, *Environ. Sci. Technol.*, 2023, **57**(34), 12901–12910, DOI: **10.1021/acs.est.3c03679**.

60 S.-M. Banyoi, T. Porseryd, J. Larsson, M. Grahn and P. Dinnétz, The Effects of Exposure to Environmentally Relevant PFAS Concentrations for Aquatic Organisms at Different Consumer Trophic Levels: Systematic Review and Meta-Analyses, *Environ. Pollut.*, 2022, **315**, 120422, DOI: **10.1016/j.envpol.2022.120422**.

61 S. Kurwadkar, J. Dane, S. R. Kanel, M. N. Nadagouda, R. W. Cawdrey, B. Ambade, G. C. Struckhoff and R. Wilkin, Per- and Polyfluoroalkyl Substances in Water and Wastewater: A Critical Review of Their Global Occurrence and Distribution, *Sci. Total Environ.*, 2021, **809**, 151003–151003, DOI: **10.1016/j.scitotenv.2021.151003**.

62 P.-F. Yan, S. Dong, K. D. Pennell and N. L. Cápiro, A Review of the Occurrence and Microbial Transformation of Per- and Polyfluoroalkyl Substances (PFAS) in Aqueous Film-Forming Foam (AFFF)-Impacted Environments, *Sci. Total Environ.*, 2024, **927**, 171883, DOI: **10.1016/j.scitotenv.2024.171883**.

63 A. Rotander, L.-M. L. Toms, L. Aylward, M. Kay and J. F. Mueller, Elevated Levels of PFOS and PFHxS in Firefighters Exposed to Aqueous Film Forming Foam (AFFF), *Environ. Int.*, 2015, **82**, 28–34, DOI: **10.1016/j.envint.2015.05.005**.

64 R. Zhang, Z. Ren, U. Bergmann, J. N. Uwayezu, I. Carabante, J. Kumpiene, T. Lejon, I. Levakov, G. Rytwo and T. Leiviskä,

Removal of Per- and Polyfluoroalkyl Substances (PFAS) from Water Using Magnetic Cetyltrimethylammonium Bromide (CTAB)-Modified Pine Bark, *J. Environ. Chem. Eng.*, 2024, **12**(5), 114006, DOI: **10.1016/j.jece.2024.114006**.

65 Z. AlYousef, S. Ayirala, M. Almubarak and D. Cha, Impact of Tailored Water Chemistry Aqueous Ions on Foam Stability Enhancement, *J. Pet. Explor. Prod. Technol.*, 2021, **11**(8), 3311–3320, DOI: **10.1007/s13202-021-01216-z**.

66 J. C. Berg, *An Introduction to Interfaces and Colloids: The Bridge to Nanoscience*, World Scientific, 2009, DOI: **10.1142/7579**.

67 M. Sochacki, P. Michorczyk and O. Vogt, Foam Fractionation as an Efficient Method for the Separation and Recovery of Surfactants and Surface-Inactive Agents: State of the Art, *ACS Omega*, 2025, **10**(1), 55–75, DOI: **10.1021/acsomega.4c08413**.

68 D. J. Burns, P. Stevenson and P. J. C. Murphy, PFAS Removal from Groundwaters Using Surface-Active Foam Fractionation, *Remediation*, 2021, **31**(4), 19–33, DOI: **10.1002/rem.21694**.

69 M. Kalbáčová, M. Verdánová, F. Mravec, T. Halasová and M. Pekař, Effect of CTAB and CTAB in the Presence of Hyaluronan on Selected Human Cell Types, *Colloids Surf., A*, 2014, **460**, 204–208, DOI: **10.1016/j.colsurfa.2013.12.048**.

70 B. Isomaa, J. Reuter and B. M. Djupsund, The Subacute and Chronic Toxicity of Cetyltrimethylammonium Bromide (CTAB), a Cationic Surfactant, in the Rat, *Arch. Toxicol.*, 1976, **35**(2), 91–96, DOI: **10.1007/BF00372762**.